第 38 卷第 4 期 分 子 催 化（中 英 文） Vol.38,No.4
2024 年 8 月 JOURNAL OF MOLECULAR CATALYSIS(CHINA) Aug. 2024

Article ID：1001-3555(2024)04-0297-12 *Articles*

Controlling Reactivity of Palladium Amides for Selective Carbonylation towards Urea and Oxamide Derivatives

WANG Jin-hui[1,2], CAO Yan-wei[1*], HE Lin[1*]

(1. State Key Laboratory for Oxo Synthesis and Selective Oxidation, Lanzhou Institute of Chemical Physics, Chinese Academy of Sciences, Lanzhou 730000, China; 2. University of Chinese Academy of Sciences, Beijing 100049, China)

Abstract: Carbonylation reactions, crucial for carbonyl group incorporation, struggle with the inherent complexity of achieving selective mono- or double-carbonylation on single substrates, often due to competing reaction pathways. Herein, our study introduces a strategy employing palladium amides, harnessing their unique reactivity control, to direct the selective carbonylation of amines for the targeted synthesis of urea and oxamide derivatives. The palladium amide structure was elucidated using single-crystal X-ray diffraction. Controlled experiments and cyclic voltammetry studies further elucidate that the oxidation of palladium amide or its insertion into a carbonyl group diverges into distinct pathways. By employing sodium percarbonate as an eco-friendly oxidant and base, we have successfully constructed a switchable carbonylation system co-catalyzed by palladium and iodide under room temperature. The utilizing strategy in this study not only facilitates effective control over reaction selectivity but also mitigates the risk of explosions, a critical safety concern in traditional carbonylation methods.

Key words: selectivity control; palladium catalysis; oxidative carbonylation; aminocarbonylation; green reagents

CLC number: O643.32 **Document code:** A **DOI:** 10.16084/j.issn1001-3555.2024.04.001

Urea and oxamide derivatives are crucial in a diverse array of fields, including biological metabolism, medical therapeutics and small molecule catalysis[1−2]. Traditionally, these compounds have been synthesized using methods involving phosgene and oxalyl chloride, which pose significant environmental and corrosive risks (Fig. 1(a))[3]. In an effort to address these concerns and improve synthesis efficiency, the field has seen a shift towards the oxidative carbonylation[4−8] of amines using carbon monoxide as a carbonyl source with various transition metal catalysts like Au[9−11], Co[12] and Pd[13−19] (Fig. 1(b)). Despite this progress, achieving selectivity between mono- and double-carbonylation remains a substantial challenge. The literature indicates that precise control over this selectivity is complex, necessitating sophisticated catalyst design and meticulous condition optimization[20−24]. Furthermore, safety concerns persist due to the potential explosiveness of oxygen-CO mixtures during these reactions.

Our design presents a reactivity control strategy of palladium amide enabled by regulating the competitive reactivity of palladium amide intermediates in the palladium-catalyzed amine carbonylation reaction (Fig. 1(c)). In this reaction, the palladium amide may undergo oxidation and future reacting with the amine, yielding a mono-carbonyl product. At higher CO concentrations, a faster subsequent CO reaction prior to reaction of the Pd amide with the amine would favor the formation of the oxamide. Based on this mechanism, we utilize sodium percarbonate (SPC), which can act as both an oxidant and a base[25]. In contrast to molecular oxygen (*e.g.* $E_{1/2}(O_2)$ *vs* NHE (Normal Hydrogen Electrode) = −1.23 V), hydrogen peroxide tends to possess stronger oxidant activities (*e.g.* $E_{1/2}(H_2O_2)$ *vs* NHE = −1.78 V)[26]. Given the superior oxidizing strength of hydrogen peroxide, the use of SPC is anticipated to positively influence the reaction progress, enabling reaction to proceed under milder, safer and more practical conditions. Although palladium-catalyzed double-carbonylation is well-known, this catalytic system has not been applied to controllable mono-carbonyl reactions of secondary amines. Our experimental results show that using SPC as a dual reagent, urea can be obtained in the yield of 61%~89% with the selectivity of 91%~99% at room temperature and 0.1 MPa CO; when the CO pressure is increased to 3 MPa, the reaction selectivity of is reversed, and oxamide can be obtained in the yield of 66%~94% with selectivity of 95%~99% (Fig. 1(d)). Consequently, SPC emerges as an eco-friendly and versatile reagent, presenting a practical alternative to traditional oxidative carbonylation methods in laboratory settings. An in-depth understanding of the reaction mechanism allows for control over the formation of targeted carbonylated products, presenting an alternative approach for more selective and safer synthesis.

1 Experimental section

1.1 General procedure

All commercially available reagents were purchased in high purity and used without further purification. All air

Received date: 2024-04-01; **Revised date:** 2024-04-27.

Foundation: The National Key Research and Development Program of Ministry of Science and Technology (No. 2022YFA1504602); Natural Science Foundation of Jiangsu Province (No. BK20211094); National Natural Science Foundation of China (No. 22302214, 21972152, U22B20137).

Biography: Wang Jin-hui(1996−), male, PhD candidate, mainly engaged in the research of carbonylation reactions and chemical synthesis. E-mail: wangjinhui_cn@163.com.

* Corresponding authors. E-mail: caoyanwei@licp.cas.cn; helin@licp.cas.cn.

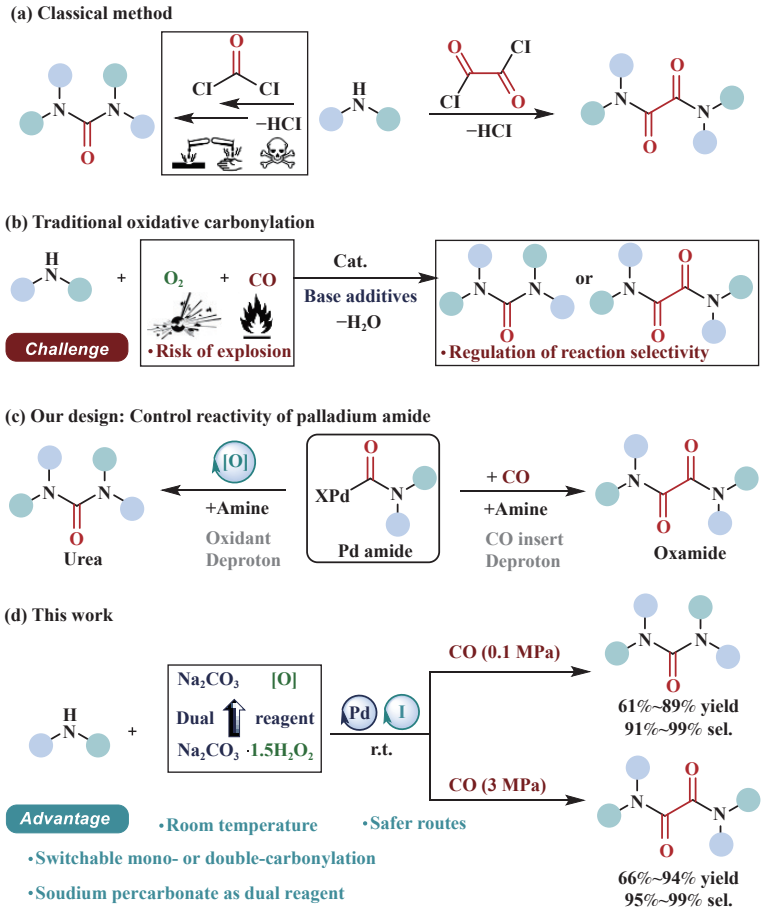

Fig.1 Comparison of various synthetic routes for urea and oxamide: (a) Phosgene route and oxalyl chloride route; (b) Traditional oxidative carbonylation using O_2 as oxidant and base additives; (c) Reactivity control strategy of palladium amide towards urea and oxamide; (d) Sodium percarbonate as dual-reagent for safer mono- and double-carbonylation of amines

sensitive manipulations were carried out using a standard Schlenk techniques or nitrogen-filled glove box under N_2 atmosphere. ^{1}H NMR and ^{13}C NMR spectra were recorded on a Bruker Avance-400 (400 MHz) spectrometer. The chemical shifts (δ) were given in 10^{-6} related to internal tetramethyl silane (TMS, δ=0 for ^{1}H NMR), $CDCl_3$ (δ=77.16 for ^{13}C NMR). All ^{1}H NMR spectra were reported in delta (δ) units, 10^{-6} downfield from the internal standard. Coupling constants are reported in Hertz (Hz). The multiplicities of signals are designated by the following abbreviations: s (singlet), d (doublet), t (triplet), q (quarter), m (multiplet), dd (doublet and doublet), dt (doublet and triplet), td (triplet and doublet). GC was performed on an Agilent 6890 instrument equipped with a HP-5 (30 m × 0.53 mm × 1.0 μm), biphenyl as an internal standard. Electron impact (EI) mass spectra were recorded on SHIMADZU GCMS-QP2010 SE mass spectrometer. High resolution mass spectra were recorded on an Agilent 1260-6530 Accurate-Mass Q-TOF LC/MS.

CAUTION: Carbon monoxide is an odorless, colorless, tasteless, poisonous gas. The permissible exposure limit (PEL) for CO set forth by OSHA is 50 mg·L^{-1} for eight hours. The immediately dangerous to life or health (IDLH) value set forth by the US National Institute for Occupational Safety and Health (NIOSH) is 1 200 mg·L^{-1}. CO handling requires a well-ventilated, operational fume hood. However, if any amount of CO is detected in the laboratory, steps must be taken to stop the leakage and potential exposure to CO.

1.2 Synthesis of Pd-Cl amide[27]

A 25 mL thick-walled Schlenk tube with a Teflon vale was charged with a magnetic stir bar, $Pd(PPh_3)_2Cl_2$ (500.0 mg, 0.71 mmol, mole ratio 1), piperidine (604.5 mg, 7.1 mmol, mole ratio 10), and then CH_3CN (10 mL) was added under N_2 atmosphere. The mixture was sealed and degassed by three freeze-pump-thaw cycles and refilled with CO (0.1 MPa). The reaction was then placed under dark condition and stirred for 2 h at room temperature. The product was filtered, washed with ethanol and Et_2O to obtain white powder (532 mg, yield 96%).

Crystals of **Pd-Cl amide** were grown by slow diffusion of hexane into CH_2Cl_2, resulting in thin colorless crystals. The structure was further confirmed by X-ray crystallography (CCDC 2322811). A suitable crystal was selected and collected on a Bruker APEX-II CCD diffractometer. The crystal was kept at −123.15 °C during data collection. Using OLEX2[28], the structure was solved with the SHELXT[29] structure solution program using Intrinsic Phasing and refined with the SHELXL[30] refinement package using Least Squares minimisation.

^{1}H NMR (400 MHz, $CDCl_3$) δ 7.78−7.34 (m, 30H), 3.69−3.62 (m, 2H), 2.46 – 2.21 (m, 2H), 1.11 – 0.84 (m, 4H), 0.50 (s, 2H).

^{31}P NMR (162 MHz, $CDCl_3$) δ 23.30, 20.13.

1.3 Procedure A for mono-carbonylation of amines

In a nitrogen-filled glove box, the reactions were carried out in a 10 mL Schlenk tube with a magnetic stirrer. As a typical run, piperidine (85.1 mg, 1 mmol, mole ratio 1) and $Na_2CO_3·1.5H_2O_2$ (314.0 mg, 2 mmol, mole ratio 2) were introduced following adding $Pd(acac)_2$ (0.01 mmol, 3.0 mg) and tetra-*n*-hexylammonium iodide $^nHex_4NI$ (0.1 mmol, 48.1 mg). The mixture was stirred for 1 min after adding THF (2 mL). After sealing with a rubber stopper, the tube was removed from the glove box and a balloon of CO was connected to the tube. Then the tube was stirred at room temperature until the piperidine had been completely consumed as judged by GC analysis. The reaction mixture was then washed with water and ethyl acetate and the organic layer was concentrated in vacuo. After removal of the solvent, the residues were purified by flash column chromatography on silica gel using hexane/ethyl acetate as eluent to afford corresponding product.

1.4 Procedure B for double-carbonylation of amines

The reactions were carried out in a 25 mL stainless steel autoclave with a magnetic stirrer. As a typical run, piperidine (85.1 mg, 1 mmol, mole ratio 1) and $Na_2CO_3·1.5H_2O_2$ (314.0 mg, 2 mmol, mole ratio 2) were introduced following adding $Pd(acac)_2$ (0.01 mmol, 3.0 mg), $^nHex_4NI$ (0.1 mmol, 48.1 mg) and THF (2 mL). The autoclave is flushed with carbon monoxide for three times and then carbon monoxide was charged to desired pressure. Then the autoclave was stirred at room temperature for 5 h. After being cooled to room temperature, the reaction pressure was reduced to the atmosphere. After removal of the solvent, the residue was purified by flash column chromatography on silica gel using ethyl acetate as eluent to afford corresponding product.

1.5 Gram-scale experiment

In a nitrogen-filled glove box, the reactions were carried out in a 100 mL Schlenk tube with a magnetic stirrer. As a typical run, piperidine (1.70 g, 20 mmol, mole ratio 1) and $Na_2CO_3·1.5H_2O_2$ (6.28 g, 40 mmol, mole ratio 2, based on amount of Na_2CO_3) were introduced following adding $Pd(acac)_2$ (0.2 mmol, 60.9 mg) and $^nHex_4NI$ (2.0 mmol, 963 mg). The mixture was stirred for 1 min after adding THF (20 mL). After sealing with a rubber stopper, the tube was removed from the glove box and a balloon of CO was connected to the tube. Then the tube was stirred at room temperature until the piperidine had been completely consumed as judged by GC analysis. The selectivity was detected by GC-MS. The reaction mixture was then washed with water and ethyl acetate and the organic layer was concentrated in vacuo. After removal of the solvent, the residue was purified by flash column chromatography on silica gel using hexane/ethyl acetate as eluent to afford corresponding product as oil (1.73 g, 73%).

1.6 Characterization data of product

The title compound was prepared according to the general procedure A and purified by column chromatography using: Hexane∶ethyl acetate = 10∶1 as eluent to afford corresponding product as light-yellow oil (79.5 mg, 81%).

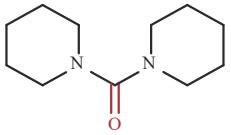

2a

^{1}H NMR (400 MHz, $CDCl_3$) δ 3.23 – 3.12 (m, 8H), 1.62 – 1.47 (m, 12H).

^{13}C NMR (101 MHz, $CDCl_3$) δ 164.85, 48.01, 25.85, 24.85.

HRMS (ESI-TOF) exact mass calculated for $[M+H]^+$ ($C_{11}H_{21}N_2O^+$) requires *m/z* 197.164 8, Found *m/z* = 197.165 0.

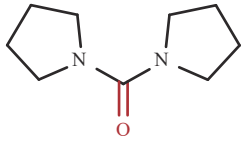

2b

Hexane∶ethyl acetate = 1∶1 as eluent to afford corresponding product as light-yellow oil (55.5 mg, 66%).

^{1}H NMR (400 MHz, $CDCl_3$) δ 3.43 – 3.30 (m, 8H), 1.89 – 1.77 (m, 8H).

^{13}C NMR (101 MHz, $CDCl_3$) δ 161.47, 47.96, 25.58.

HRMS (ESI-TOF) exact mass calculated for $[M+H]^+$ ($C_9H_{17}N_2O^+$) requires *m/z* 169.133 5, Found *m/z* = 169.133 1.

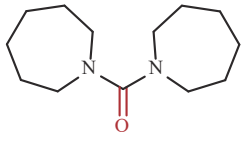

2c

Hexane∶ethyl acetate = 1∶1 as eluent to afford corresponding product as light-yellow oil (83.0 mg, 74%).

^{1}H NMR (400 MHz, $CDCl_3$) δ 3.31 (t, 8H), 1.79 – 1.67 (m, 8H), 1.64 – 1.49 (m, 8H).

^{13}C NMR (101 MHz, $CDCl_3$) δ 165.78, 49.46, 28.74, 27.53.

HRMS (ESI-TOF) exact mass calculated for $[M+H]^+$ ($C_{13}H_{25}N_2O^+$) requires *m/z* 225.196 1, Found *m/z* = 225.196 3.

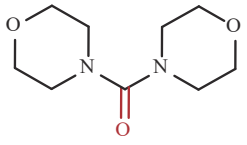

2d

Hexane∶ethyl acetate = 1∶1 as eluent to afford corresponding product as white powder (68.1 mg, 68%).

^{1}H NMR (400 MHz, $CDCl_3$) δ 3.68 (t, 8H), 3.28 (t, 8H).

^{13}C NMR (101 MHz, $CDCl_3$) δ 163.83, 66.64, 47.26.

HRMS (ESI-TOF) exact mass calculated for $[M+Na]^+$ ($C_9H_{16}N_2O_3Na^+$) requires *m/z* 223.105 3, Found *m/z* = 223.105 5.

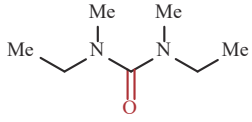

2e

Hexane∶ethyl acetate = 1∶1 as eluent to afford corresponding product as light-yellow oil (49.0 mg, 68%).

^{1}H NMR (400 MHz, $CDCl_3$) δ 3.18 (q, J = 7.1 Hz, 4H), 2.77 (s, 6H), 1.14 (t, J = 7.1 Hz, 6H).

^{13}C NMR (101 MHz, $CDCl_3$) δ 165.52, 45.17, 35.74,

12.85.

HRMS (ESI-TOF) exact mass calculated for $[M+H]^+$ ($C_7H_{17}N_2O^+$) requires *m/z* 145.133 5, Found *m/z* = 145.133 6.

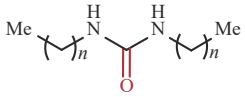

2f, *n* = 4

Hexane∶ethyl acetate = 1∶1 as eluent to afford corresponding product as white powder (89.1 mg, 89%).

^{1}H NMR (400 MHz, $CDCl_3$) *δ* 5.67 (s, 2H), 3.13 (t, *J* = 6.7 Hz, 4H), 1.47 (m, 4H), 1.35 – 1.25 (m, 8H), 0.89 (t, *J* = 6.9 Hz, 6H).

^{13}C NMR (101 MHz, $CDCl_3$) *δ* 159.47, 40.32, 30.21, 29.22, 22.52, 14.05.

HRMS (ESI-TOF) exact mass calculated for $[M+H]^+$ ($C_{11}H_{25}N_2O^+$) requires *m/z* 201.196 1, Found *m/z* = 201.196 3.

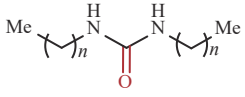

2g, *n* = 5

Hexane∶ethyl acetate = 1∶1 as eluent to afford corresponding product as white powder (99.3 mg, 87%).

^{1}H NMR (400 MHz, $CDCl_3$) *δ* 5.53 (s, 2H), 3.12 (t, *J* = 7.1 Hz, 4H), 1.59 – 1.39 (m, 4H), 1.35 – 1.20 (m, 12H), 0.88 (t, *J* = 6.8 Hz, 6H).

^{13}C NMR (101 MHz, $CDCl_3$) *δ* 159.38, 40.44, 31.74, 30.50, 26.79, 22.70, 14.11.

HRMS (ESI-TOF) exact mass calculated for $[M+H]^+$ ($C_{13}H_{29}N_2O^+$) requires *m/z* 229.227 4, Found *m/z* = 229.227 4.

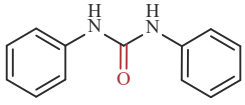

2h

Hexane∶ethyl acetate = 1∶1 as eluent to afford corresponding product as light-yellow powder (64.7 mg, 61%).

^{1}H NMR (400 MHz, DMSO-d_6) *δ* 8.67 (s, 2H), 7.47 (d, *J* = 7.7 Hz, 4H), 7.28 (t, *J* = 7.9 Hz, 4H), 6.97 (t, *J* = 7.3 Hz, 2H).

^{13}C NMR (101 MHz, DMSO-d_6) *δ* 152.56, 139.74, 128.81, 121.82, 118.19.

HRMS (ESI-TOF) exact mass calculated for $[M+Na]^+$ ($C_{13}H_{12}N_2ONa^+$) requires *m/z* 235.084 2, Found *m/z* = 235.084 7.

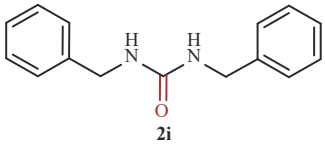

2i

Hexane∶ethyl acetate = 1∶1 as eluent to afford corresponding product as white powder (76.9 mg, 64%).

^{1}H NMR (400 MHz, DMSO-d_6) *δ* 7.35 – 7.19 (m, 10H), 6.48 – 6.40 (m, 2H), 4.33 – 4.13 (m, 4H).

^{13}C NMR (101 MHz, DMSO-d_6) *δ* 158.20, 140.96, 128.27, 127.03, 126.60, 43.04.

HRMS (ESI-TOF) exact mass calculated for $[M+H]^+$ ($C_{15}H_{17}N_2O^+$) requires *m/z* 241.133 5, Found *m/z* = 241.133 8.

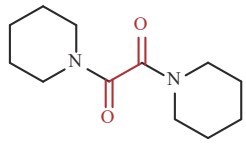

3a

The title compound was prepared according to the general procedure B and purified by column chromatography using: Hexane∶ethyl acetate = 1∶1 as eluent to afford corresponding product as light-yellow powder (103.1 mg, 92%).

^{1}H NMR (400 MHz, $CDCl_3$) *δ* 3.58 (t, 4H), 3.34 (t, 4H), 1.72 – 1.56 (m, 12H).

^{13}C NMR (101 MHz, $CDCl_3$) *δ* 163.55, 47.23, 41.75, 26.45, 25.34, 24.43.

HRMS (ESI-TOF) exact mass calculated for $[M+H]^+$ ($C_{12}H_{21}N_2O_2^+$) requires *m/z* 225.159 8, Found *m/z* = 225.159 6.

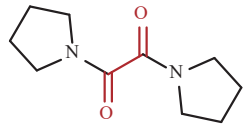

3b

Hexane∶ethyl acetate = 1∶1 as eluent to afford corresponding product as white solid (92.2 mg, 94%).

^{1}H NMR (400 MHz, $CDCl_3$) *δ* 3.63 – 3.31 (m, 8H), 2.00 – 1.88 (m, 8H).

^{13}C NMR (101 MHz, $CDCl_3$) *δ* 163.09, 46.68, 44.84, 25.65, 23.93.

HRMS (ESI-TOF) exact mass calculated for $[M+H]^+$ ($C_{10}H_{17}N_2O_2^+$) requires *m/z* 197.128 5, Found *m/z* = 197.129 1.

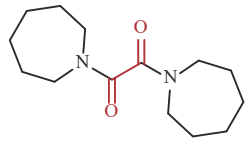

3c

Hexane∶ethyl acetate = 1∶1 as eluent to afford corresponding product as colorless oil (90.8 mg, 72%).

^{1}H NMR (400 MHz, $CDCl_3$) *δ* 3.60 – 3.48 (m, 4H), 3.45 – 3.37 (m, 4H), 1.84 – 1.71 (m, 8H), 1.67 – 1.56 (m, 8H).

^{13}C NMR (101 MHz, $CDCl_3$) *δ* 165.26, 47.99, 44.58, 28.93, 27.90, 27.00, 26.41.

HRMS (ESI-TOF) exact mass calculated for $[M+H]^+$ ($C_{14}H_{25}N_2O_2^+$) requires *m/z* 253.191 1, Found *m/z* = 253.191 4.

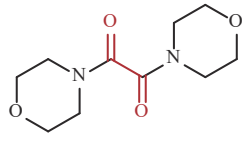

3d

Ethyl acetate as eluent to afford corresponding product as white powder (84.4 mg, 74%).

^{1}H NMR (400 MHz, $CDCl_3$) *δ* 3.75 – 3.69 (m, 8H), 3.66 (t, 4H), 3.45 (t, 4H).

^{13}C NMR (101 MHz, $CDCl_3$) δ 162.81, 66.89, 66.59, 46.58, 41.51.

HRMS (ESI-TOF) exact mass calculated for $[M+H]^+$ ($C_{10}H_{17}N_2O_4^+$) requires *m/z* 229.118 3, Found *m/z* = 229.118 8.

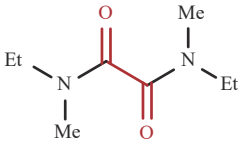

3e

Hexane∶ethyl acetate = 1∶1 as eluent to afford corresponding product as light-yellow oil (76.6 mg, 89%).

^{1}H NMR (400 MHz, $CDCl_3$) δ 3.47 (q, J = 7.2 Hz, 2H), 3.31 (q, J = 7.1 Hz, 2H), 2.97 (d, J = 1.2 Hz, 3H), 2.96 (d, J = 1.7 Hz, 3H), 1.22 (t, J = 7.1 Hz, 3H), 1.18 (t, J = 7.2 Hz, 3H).

^{13}C NMR (101 MHz, $CDCl_3$) δ 165.05, 164.72, 44.86, 44.75, 40.95, 40.90, 34.52, 34.25, 30.79, 30.75, 13.46, 13.42, 11.87, 11.84.

HRMS (ESI-TOF) exact mass calculated for $[M+H]^+$ ($C_8H_{17}N_2O_2^+$) requires *m/z* 173.128 5, Found *m/z* = 173.129 0.

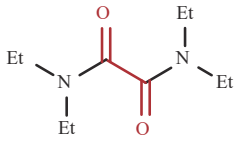

3f

Hexane∶ethyl acetate = 1∶1 as eluent to afford corresponding product as white solid (76.6 mg, 89%).

^{1}H NMR (400 MHz, $CDCl_3$) δ 3.45 (q, J = 7.2 Hz, 4H), 3.29 (q, J = 7.1 Hz, 4H), 1.25 – 1.16 (m, 12H).

^{13}C NMR (101 MHz, $CDCl_3$) δ 164.70, 42.26, 38.25, 13.95, 12.54.

HRMS (ESI-TOF) exact mass calculated for $[M+H]^+$ ($C_{10}H_{21}N_2O_2^+$) requires *m/z* 201.159 8, Found *m/z* = 201.160 1.

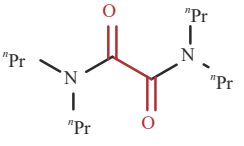

3g

Hexane∶ethyl acetate = 1∶1 as eluent to afford corresponding product as light-yellow oil (85.9 mg, 67%).

^{1}H NMR (400 MHz, $CDCl_3$) δ 3.34 (t, 4H), 3.15 (t, 4H), 1.70 – 1.56 (m, 8H), 0.94 (t, J = 7.4 Hz, 6H), 0.88 (t, J = 7.4 Hz, 6H).

^{13}C NMR (101 MHz, $CDCl_3$) δ 165.15, 49.65, 45.37, 21.66, 20.38, 11.33, 11.09.

HRMS (ESI-TOF) exact mass calculated for $[M+H]^+$ ($C_{14}H_{29}N_2O_2^+$) requires *m/z* 257.222 4, Found *m/z* = 257.223 1.

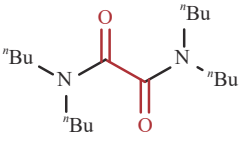

3h

Hexane∶ethyl acetate = 1∶1 as eluent to afford corresponding product as light-yellow oil (103.1 mg, 66%).

^{1}H NMR (400 MHz, $CDCl_3$) δ 3.37 (t, 4H), 3.17 (t, 4H), 1.64 – 1.50 (m, 8H), 1.38 – 1.24 (m, 8H), 0.96 – 0.88 (m, 12H).

^{13}C NMR (101 MHz, $CDCl_3$) δ 165.14, 47.87, 43.60, 30.60, 29.34, 20.26, 20.09, 13.87, 13.76.

HRMS (ESI-TOF) exact mass calculated for $[M+H]^+$ ($C_{18}H_{37}N_2O_2^+$) requires *m/z* 313.285 0, Found *m/z* = 313.285 4.

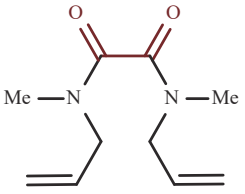

3i

Hexane∶ethyl acetate = 3∶1 as eluent to afford corresponding product as light-yellow oil (80.5 mg, 82%).

^{1}H NMR (400 MHz, $CDCl_3$) δ 5.87 – 5.71 (m, 2H), 5.33 – 5.20 (m, 4H), 4.03 (t, J = 6.3 Hz, 2H), 3.88 (dd, J = 10.9, 6.0 Hz, 2H), 2.95 (t, J = 0.0 Hz, 6H).

^{13}C NMR (101 MHz, $CDCl_3$) δ 164.93, 164.89, 164.64, 164.58, 132.34, 132.17, 131.44, 131.43, 118.91, 118.47, 118.38, 52.68, 52.46, 48.39, 48.30, 34.66, 34.31, 31.21, 31.14.

HRMS (ESI-TOF) exact mass calculated for $[M+H]^+$ ($C_{10}H_{17}N_2O_2^+$) requires *m/z* 197.128 5, Found *m/z* = 197.128 7.

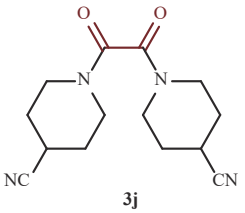

3j

Ethyl acetate as eluent to afford corresponding product as white solid (112.3 mg, 82%).

^{1}H NMR (400 MHz, $CDCl_3$) δ 3.84 – 3.31 (m, 8H), 3.10 – 2.92 (m, 2H), 2.06 – 1.80 (m, 8H).

^{13}C NMR (101 MHz, $CDCl_3$) δ 162.64, 120.39, 44.19, 44.07, 38.91, 38.78, 28.73, 28.68, 27.89, 27.84, 26.18, 26.12.

HRMS (ESI-TOF) exact mass calculated for $[M+H]^+$ ($C_{14}H_{19}N_4O_2^+$) requires *m/z* 275.150 3, Found *m/z* = 275.148 9.

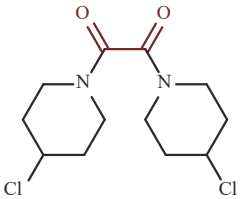

3k

Ethyl acetate as eluent to afford corresponding product as white solid (111.4 mg, 79%).

^{1}H NMR (400 MHz, $CDCl_3$) δ 4.46 – 4.33 (m, 2H), 3.83 – 3.58 (m, 6H), 3.43 – 3.28 (m, 2H), 2.29 – 2.04 (m, 4H), 1.98 – 1.81 (m, 4H).

^{13}C NMR (101 MHz, $CDCl_3$) δ 162.92, 162.89, 56.00, 55.91, 43.05, 42.93, 37.73, 37.61, 34.87, 34.79, 33.96, 33.90.

HRMS (ESI-TOF) exact mass calculated for $[M+Na]^+$

($C_{12}H_{18}Cl_2N_2O_2Na^+$) requires *m/z* 315.063 8, Found *m/z* = 315.064 3.

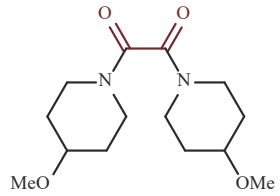

3l

Ethyl acetate as eluent to afford corresponding product as colorless oil (88.1 mg, 62%).

^{1}H NMR (400 MHz, $CDCl_3$) δ 3.88 – 3.75 (m, 2H), 3.62 – 3.45 (m, 6H), 3.36 (s, 6H), 3.28 – 3.16 (m, 2H), 2.00 – 1.80 (m, 4H), 1.74 – 1.57 (m, 4H).

^{13}C NMR (101 MHz, $CDCl_3$) δ 163.35, 163.32, 74.74, 55.90, 43.11, 37.73, 30.98, 30.95, 29.82, 29.78.

HRMS (ESI-TOF) exact mass calculated for $[M+Na]^+$ ($C_{14}H_{24}N_2O_4Na^+$) requires *m/z* 307.162 8, Found *m/z* = 307.162 8.

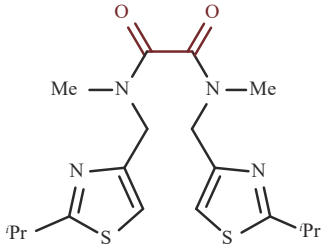

3m

Ethyl acetate as eluent to afford corresponding product as white solid (149.7 mg, 76%).

^{1}H NMR (400 MHz, $CDCl_3$) δ 7.15 (d, *J* = 30.0 Hz, 1H), 7.06 (d, *J* = 4.7 Hz, 1H), 4.71 (d, *J* = 11.7 Hz, 2H), 4.62 – 4.57 (m, 2H), 3.32 – 3.18 (m, 2H), 3.13 – 3.05 (m, 3H), 3.04 – 2.97 (m, 3H), 1.42 – 1.29 (m, 12H).

^{13}C NMR (101 MHz, $CDCl_3$) δ 178.50, 178.41, 178.28, 178.26, 165.20, 165.10, 165.05, 164.94, 150.58, 150.54, 150.43, 115.68, 115.48, 114.75, 114.34, 50.01, 49.52, 46.02, 45.55, 35.74, 35.06, 33.17, 33.14, 31.81, 31.57, 23.10, 23.05.

HRMS (ESI-TOF) exact mass calculated for $[M+Na]^+$ ($C_{18}H_{26}N_4O_2S_2Na^+$) requires *m/z* 417.138 9, Found *m/z* = 417.139 0.

2 Results and discussion

At the beginning, inspired by previous literature, we focused on the role of **Pd-Cl amide** in the carbonylation of amines (Fig. 2)[17, 27]. The synthesis of **Pd-Cl amide** was achieved by reacting $Pd(PPh_3)_2Cl_2$ with carbon monoxide (CO) and piperidine (**1a**) under ambient conditions. High-resolution mass spectrometry (HR-MS) confirmed the formation of the Pd amide species with an *m/z* of 742.161 4, corresponding to the **Pd$^+$ amide** ion. Single crystal X-ray diffraction revealed a four-coordinate palladium complex (Fig. 2(a)). The bond angles between Pd—C and P1, Pd—C and P2 are 89.7° and 88.3°, respectively. The Pd—C bond length is 0.200 1 nm, and the C—O bond length is 0.122 7 nm. Infrared (IR) spectra further validated the formation of **Pd-Cl amide**, with characteristic absorption bands at 1 585 cm^{-1} and 1 598 cm^{-1}, indicative of the CO stretch in the amide complex, absent in the spectrum of the starting $Pd(PPh_3)_2Cl_2$ (Fig. 2(b)).

Further cyclic voltammetry (CV) studies were employed to dissect the redox characteristics of the **Pd-Cl amide** and other possible catalytic species, providing insights into the electron transfer processes that underpin the carbonylation reaction (Fig. 3). The CV analysis implies that iodide ions may be preferentially oxidized over **Pd-Cl amide** and Pd(0) species, which could affect the course of the catalytic reaction and the formation of products (Fig. 3(a)-(i)). Furthermore, the mixture of **Pd-Cl amide** and ^{n}Hex$_4$NI showed an obvious peak at 0.7 V,

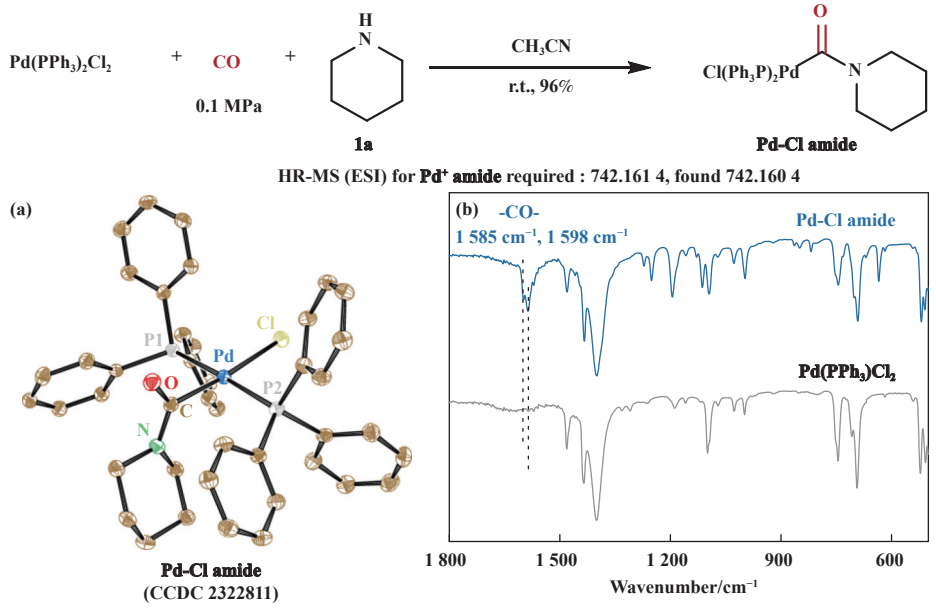

Fig.2 Synthesis and characterization of **Pd-Cl amide**: (a) X-ray crystal structure: Displacement ellipsoids are drawn at the 30% probability level, hydrogen atoms are omitted for clarity; (b) IR spectra

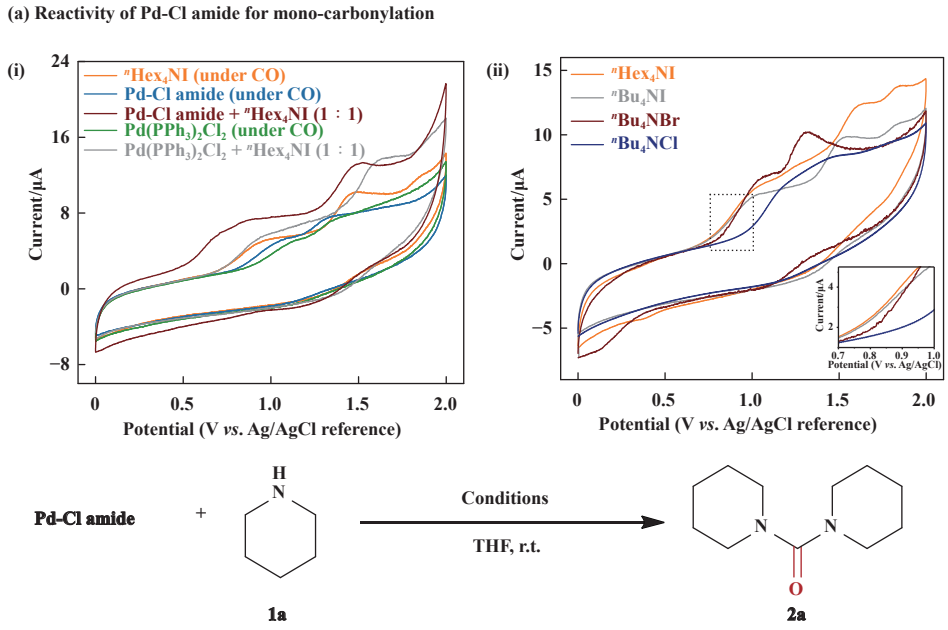

Entry	Conditions	GC yield of 2a/%
1	$Na_2CO_3 \cdot 1.5H_2O_2$ mole ratio 20, $^nHex_4NI$ mole ratio 10	17
2	$Na_2CO_3 \cdot 1.5H_2O_2$ mole ratio 20	n.d.
3	$^nHex_4NI$ mole ratio 10	n.d.
4	I_2 mole ratio 4	53

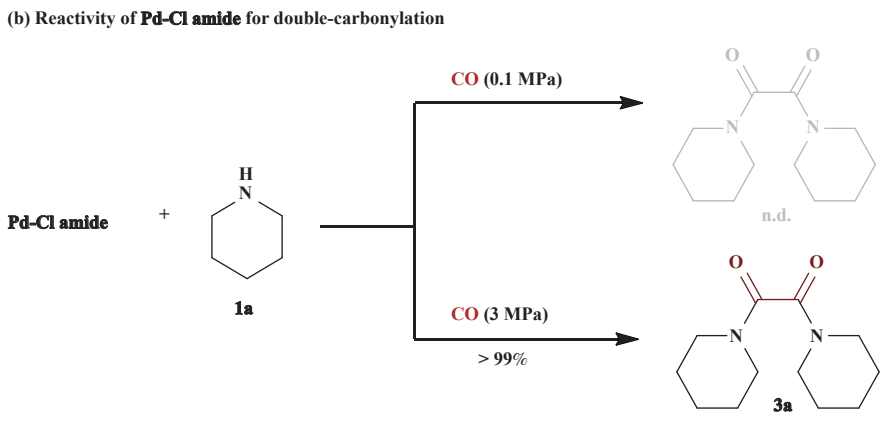

Fig.3 CV profiling and reactivity of **Pd-Cl amide**: (a) Synthesis of urea from **Pd-Cl amide**, (ⅰ) CV curves of various catalytic species (0.12 mmol·L^{-1}) in CH_2Cl_2 : CH_3CN (1 : 10, volume fraction), (ⅱ) CV curves of various ammonium salts (0.13 mmol·L^{-1}) in CH_3CN; (b) synthesis of oxamide from **Pd-Cl amide**

indicating that the oxidation was generated by the reduction of I_2 under 0.1 MPa CO pressure[31]. Further studies found that when **Pd-Cl amide** was mixed directly with iodine, an increase in chemical shifts was clearly seen in the ^{31}P NMR spectra[32−33], indicating that the palladium was further oxidized and the electronegativity of the palladium increased. In catalytic oxidative carbonylation reactions, the preferential oxidation of iodide ions could lead to the formation of iodine species, which may further interact with other reactants, such as Pd amide and Pd(0) species thus influencing the efficiency and selectivity of the entire oxidative carbonylation cycle[14, 34−38]. The CV analysis revealed discernible electrochemical signatures for various ammonium salts, with the voltammetric profiles suggesting that anion and alkyl chain length significantly

influences their redox behavior (Fig. 3(a)-(ii)). Different onset potentials for oxidation were observed, with $^{n}Hex_4NI$ exhibiting easier oxidation. Subsequent reactivity studies of the **Pd-Cl amide** complex in mono-carbonylation reactions revealed its capability to transform amine **1a** into the corresponding **2a** under various conditions. When sodium percarbonate and $^{n}Hex_4NI$ were used in a 2 : 1 mole ratio, a modest 17% GC yield of **2a** was observed (Entry 1). In the absence of $^{n}Hex_4NI$, no desired product was detected (n.d.), highlighting the importance of this additive (Entry 2). Likewise, the use of $^{n}Hex_4NI$ alone did not lead to product formation, suggesting that both the oxidant and the additive are crucial for the reaction to proceed (Entry 3). Notably, the inclusion of iodine (I_2) as an oxidant led to a significantly enhanced yield of 53%, indicating that iodine may play a role in activating the **Pd-Cl amide** towards **2a** (Entry 4). For double-carbonylation reactions, the **Pd-Cl amide** complex demonstrated exceptional selectivity in the presence of a higher CO pressure (3.0 MPa), converting amine **1a** exclusively to the double-carbonylated product **3a** with a yield of over 99% (Fig. 3(b)). This stark contrast in reactivity under different CO pressures suggests that the **Pd-Cl amide** complex can be finely tuned to favor either mono- or double-carbonylation based on the reaction conditions. This information is crucial for understanding the catalytic mechanism and for further optimization of the catalytic system.

After having confirmed the successful control of the palladium amide reactivity, our next objective was to apply it in the oxidative carbonylation of amines. To demonstrate the viability of the strategy, we evaluate the outcomes of various systems in the carbonylation of piperidine at room temperature using palladium catalyst (0.01 mmol) and $^{n}Hex_4NI$ (0.10 mmol) (Table 1). Notably, the use of sodium percarbonate (SPC) as an oxidant yielded moderate to high yields of the desired carbonylation product **2a**, with the highest yield of 86% being achieved under 0.1 MPa CO for 12 h (Entry 1 to 3). Conversely, using sodium perborate ($NaBO_3$) alone resulted in significantly lower yields (Entry 4), but when combined with Na_2CO_3, the yield and selectivity towards mono-carbonylation improved within 5 h (Entry 5), underscoring the synergistic effect of the base in enhancing catalytic activity. Since sodium percarbonate is solid peroxygen compounds, it will slowly release the hydrogen peroxide and the basic sodium carbonate in solution.[39] At the same time, the slow release of anhydrous hydrogen peroxide will be more favorable to the reaction as sodium percarbonate is not soluble under THF in the system. When the reaction was conducted with H_2O_2 (30%) and Na_2CO_3 as the oxidant and base, no desired product was detected (n.d.) (Entry 6). The use of potassium persulfate ($K_2S_2O_8$) and *tert*-butyl hydroperoxide (TBHP) resulted in significantly lower 21 and 12 yields of **2a** (Entry 7 and 8). We tested the results using $^{n}Bu_4NBr$ and $^{n}Bu_4NCl$ in place of $^{n}Hex_4NI$ and no product formation was detected, which also demonstrates the importance of the iodide ion in the reaction (Entry 9 and 10). This is in line with the previously mentioned results of using cyclic voltammetry to test different quaternary ammonium salts, $^{n}Hex_4NI$ is more susceptible to oxidation. (Fig. 3 (a)-(ii)), and consequently the system is the most reactive when $^{n}Hex_4NI$ is used as a redox promoter.

Table 1 Evaluation of catalytic performance over various systems in the carbonylation of piperidine[a]

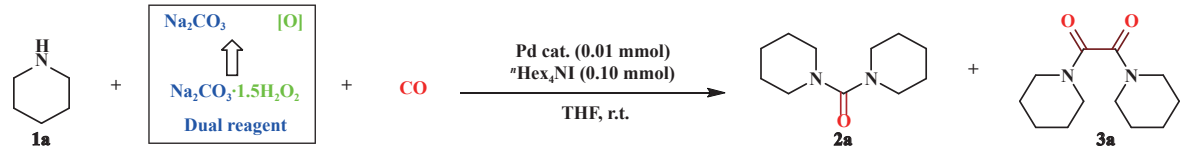

Entry	Pd cat.	Conditions	CO/MPa	**2a** yield/%	**3a** yield/%	**2a** : **3a**
1	$Pd(PPh_3)Cl_2$	$Na_2CO_3·1.5H_2O_2$	0.1	36	7	84 : 16
2	$Pd(acac)_2$	$Na_2CO_3·1.5H_2O_2$	0.1	50	4	93 : 7
3[b]	$Pd(acac)_2$	$Na_2CO_3·1.5H_2O_2$	0.1	86	9	91 : 9
4	$Pd(acac)_2$	$NaBO_3$	0.1	1	6	12 : 88
5[c]	$Pd(acac)_2$	$NaBO_3 + Na_2CO_3$	0.1	9	2	82 : 18
6[c]	$Pd(acac)_2$	$H_2O_2 + Na_2CO_3$	0.1	n.d.	n.d.	–
7[c]	$Pd(acac)_2$	$K_2SO_8 + Na_2CO_3$	0.1	21	1	96 : 4
8[c]	$Pd(acac)_2$	$TBHP + Na_2CO_3$	0.1	12	n.d.	100 : 0
9[d]	$Pd(acac)_2$	$Na_2CO_3·1.5H_2O_2$	0.1	n.d.	n.d.	–
10[e]	$Pd(acac)_2$	$Na_2CO_3·1.5H_2O_2$	0.1	n.d.	n.d.	–
11[b]	$Pd(acac)_2$	Air (0.1 MPa)	0.1	n.d.	23	0 : 100
12[b, f]	$Pd(acac)_2$	Air (0.5 MPa)	3.0	n.d.	95	0 : 100
13[f]	$Pd(acac)_2$	$Na_2CO_3·1.5H_2O_2$	3.0	3	94	3 : 97

a. Reaction conditions: piperidine (85.2 mg, 1 mmol, mole ratio 1), Pd species (0.01 mmol), $^{n}Hex_4NI$ (0.10 mmol), oxidant (mole ratio 3), CO (0.1 MPa) and THF (3.0 mL) at room temperature for 5 h. The yields and selectivity of various products were detected by GC using biphenyl as an internal standard;

b. Reaction for 12 h; c. Oxidant (mole ratio 3), Na_2CO_3 (mole ratio 2); d. $^{n}Bu_4NBr$ instead of $^{n}Hex_4NI$;

e. $^{n}Bu_4NCl$ instead of $^{n}Hex_4NI$; f. Reaction with CO (3.0 MPa).

Furthermore, the reaction atmosphere was found to be a critical parameter. Under ambient air, the system favored double-carbonylation exclusively (Entry 11). The yield of **3a** is further amplified to 95% with increased CO pressure (Entry 12). A noteworthy observation is that increasing the CO pressure to 3.0 MPa in the presence of SPC as an oxidant drastically increased the selectivity towards the doubly carbonylated product **3a** with 97% selectivity (Entry 13). These results suggest that the choice of oxidant, the presence of a base, and the reaction atmosphere play pivotal roles in dictating the yield and selectivity of carbonylation reactions. The use of SPC under low CO pressure appears to be the most effective condition among those tested, providing a promising route for the selective synthesis of the mono-carbonylated product. When the reaction pressure increases, the reaction selectivity is reversed and the reaction becomes more likely to obtain oxamide products.

The scope of the optimized carbonylation conditions was extensively investigated, with various amines subjected to both mono- and double-carbonylation reactions (Fig. 4). For mono-carbonylation, the reaction exhibits considerable versatility. Piperidine (**1a**) underwent carbonylation with an excellent yield

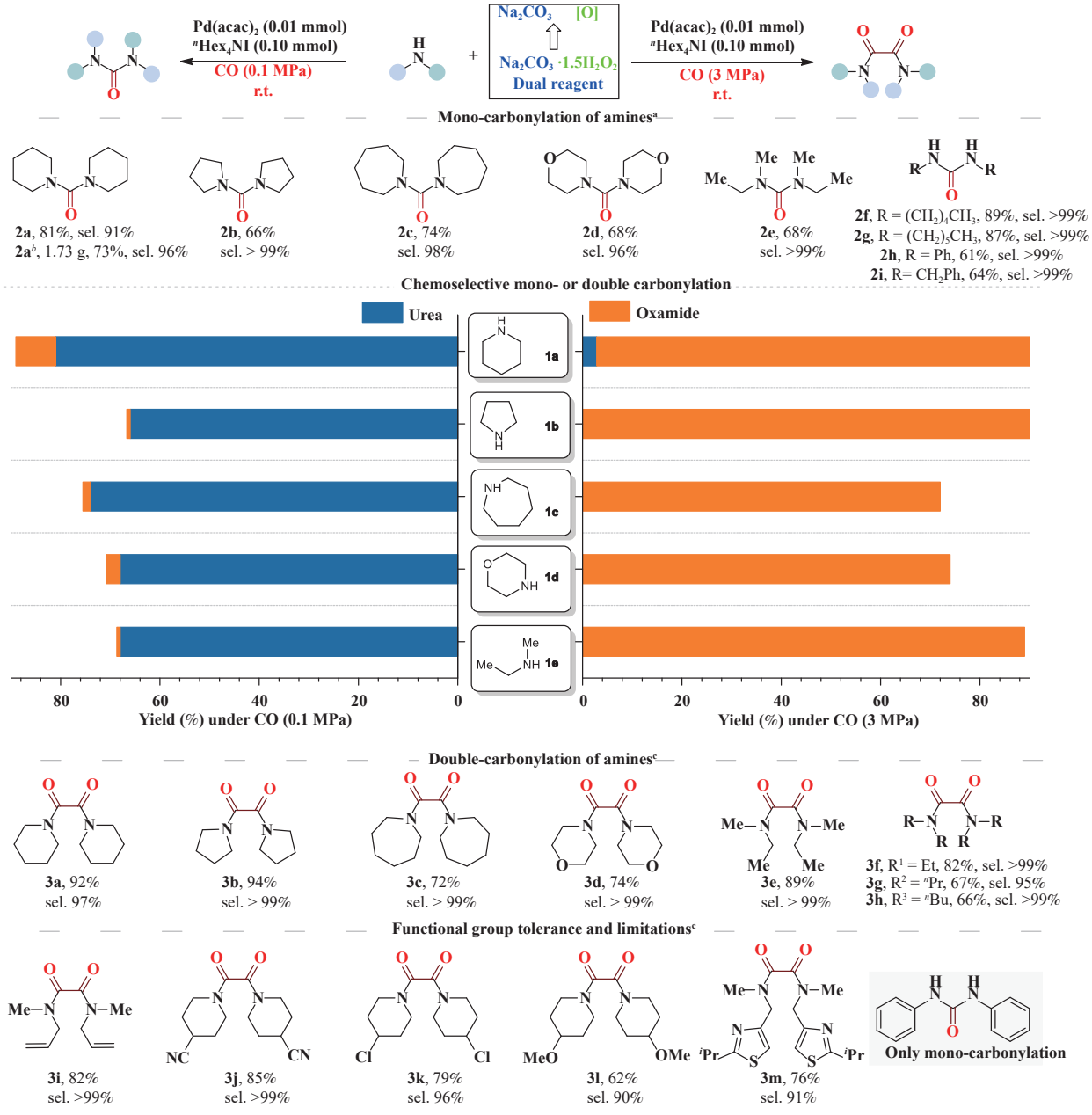

Fig.4 Scope of $Na_2CO_3{\cdot}1.5H_2O_2$ as dual-reagent in palladium-catalyzed carbonylation of amines

a. Reaction conditions: amine (1 mmol), $Pa(acac)_2$ (0.01 mmol), $^nHex_4NI$ (0.1 mmol), SPC (2 mmol, 314.0 mg, mole ratio 2 based on amount of Na_2CO_3), CO (0.1 MPa) and THF (3.0 mL) at room temperature for 12 h. Isolated yield. The chemoselectivity of mono- or double-carbonylation was determined by GC-MS; b. Piperidine (1.70 g, 20 mmol), SPC (6.28 g, 40 mmol), $Pd(acac)_2$ (0.2 mmol) and $^nHex_4NI$ (2.0 mmol); c. CO (3.0 MPa), 5 h.

of 81%. Large-scale synthesis confirmed the reaction's robustness, producing 1.73 g of the product from a 20 mmol starting amount of **1a**. Other cyclic amines, such as pyrrolidine (**1b**), azepane (**1c**) and morpholine (**1d**), also provided 66%~74% yields, respectively. The reaction was further tested on *N*-methyl-ethylamine (**1e**), which produced a 68% yield. Primary amines (**2f**−**2i**), including alkyl, aromatic and aromatic amines were also successfully carbonylated, with yields ranging from 64% to 89%, demonstrating the applicability of our method. Under the optimized conditions for dicarbonylation, we observed similarly encouraging results. Piperidine (**1a**) achieved an exceptional yield of 92%, while pyrrolidine (**1b**), azepane (**1c**) and morpholine (**1d**) resulted in a 72%~94% yield. Moreover, the reaction was tolerant of different alkyl substituents on the nitrogen atom, as evidenced by the yields of 66%~89% for **3e**−**3h**, with selectivity exceeding 95%. These findings demonstrate that the developed catalytic system possesses a broad substrate scope and can facilitate both mono- and double-carbonylation reactions of secondary amines with high efficiency. The reaction has a wide functional group tolerance and can be applied to amines with vinyl, cyano, chloro, methoxy, and thiazole rings (**3i**−**3m**). However, aniline yielded only a mono-carbonyl product even under high CO pressure. This versatility is indicative of the potential applicability of this catalytic system in the synthesis of a diverse array of amide compounds, which could have significant implications in the pharmaceutical and materials science sectors.

Drawing on our experimental results and relevant literature, we propose a tentative concerted catalytic mechanism for both mono- and double-carbonylation reactions (Fig. 5)[25, 39−41]. In the mono-carbonylation cycle, sodium percarbonate, along with I^-, activates the Pd amide complex. This complex then interacts with the amine, facilitating urea formation. Here, sodium percarbonate also serves as a base, deprotonating intermediates to aid the carbonylation step. For double-carbonylation, under high CO pressure, the activated Pd amide complex undergoes a second CO insertion step, leading to oxamide production. Sodium percarbonate again fulfills a dual role, both re-oxidizing the palladium center and providing the base for deprotonation. The combined spectroscopic and reactivity data presented in this study provide compelling evidence for the active role of the **Pd-Cl amide** complex in the catalytic cycle of amine carbonylation. The ability to control the selectivity of the reaction by varying the CO pressure and the use of ^{n}Hex$_4$NI offers a valuable insight into the mechanistic aspects of amide bond formation using palladium catalysis.

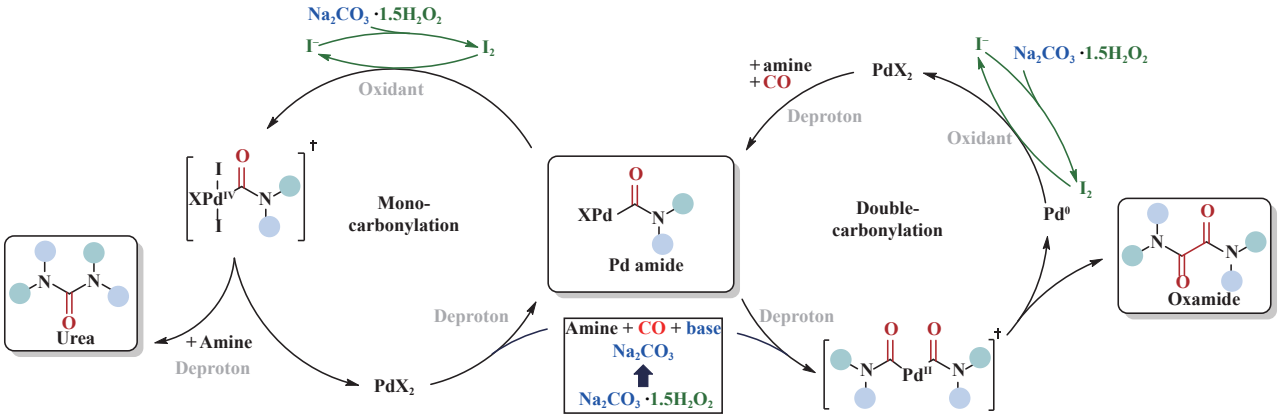

Fig.5 Proposed mechanism for selective mono- and double-carbonylation of amines towards urea and oxamide derivative

3 Conclusions

In this work, we have established a novel approach for selective carbonylation using reactivity control strategy of palladium amides, effectively addressing the challenge of achieving specific mono- or dicarbonylation on single substrates. Our study provides an in-depth understanding of palladium amide reactivity, illustrated by controlled experiments and cyclic voltammetry studies. We demonstrate that, under varying CO pressures, the use of sodium percarbonate as an oxidant and base enables a switchable carbonylation system, yielding urea with up to 89% and oxamide with up to 94% yield, showcasing impressive selectivity (91%~99% for urea, 95%~99% for oxamide). This approach not only enhances the efficiency of the carbonylation process but also significantly reduces the risk of explosions, a notable concern in traditional methods. We anticipate that this work will inspire further exploration in the field of catalysis chemistry, potentially leading to more advanced and sustainable chemical synthesis processes.

References

[1] Ghosh A K, Brindisi M. Urea derivatives in modern drug discovery and medicinal chemistry[J]. *J Med Chem*, 2020, **63**(6): 2751−2788.

[2] Ronchetti R, Moroni G, Carotti A, *et al*. Recent advances in urea- and thiourea-containing compounds: Focus on innovative approaches in medicinal chemistry and organic synthesis[J]. *RSC Med Chem*, 2021, **12**(7): 1046−1064.

[3] Bigi F, Maggi R, Sartori G. Selected syntheses of ureas through phosgene substitutes[J]. *Green Chem*, 2000, **2**(4): 140−148.

[4] Wu X F, Neumann H, Beller M. Synthesis of heterocycles *via* palladium-catalyzed carbonylations[J]. *Chem Rev*, 2013, **113**(1): 1−35.

[5] Ragaini F. Away from phosgene: Reductive carbonylation of nitroarenes and oxidative carbonylation of amines, understanding the mechanism to improve performance[J]. *Dalton Trans*, 2009, **2009**(32): 6251−6266.

[6] Díaz D J, Darko A K, McElwee-White L. Transition metal-catalyzed oxidative carbonylation of amines to ureas[J]. *Eur J Org Chem*, 2007, **2007**(27): 4453−4465.

[7] a. Liu Q, Zhang H, Lei A. Oxidative carbonylation reactions: Organometallic compounds (R-M) or hydrocarbons (R-H) as nucleophiles[J]. *Angew Chem Int Ed*, 2011, **50**(46): 10788−10799.
b. Xu P C, Liu Y Y, Qian B, *et al*. Palladium-catalyzed

hydroaminocarbonylation of alkene with triazine[J]. *J Mol Catal (China)*, 2023, **37**(3): 225-233.
c. Cao Y W, Zhang X H, He L. Recent advance in synthesis of urea by oxidative carbonylation of amine[J]. *J Mol Catal (China)*, 2020, **34**(2): 182−192.
d. Huang Z J, Wu S X, LI Y H. Recent advances on regioselectivity of carbonylation reaction[J]. *J Mol Catal (China)*, 2019, **33**(6): 578−591.

[8] Yuan Y, Wu X F. Generation and transformation of *α*-oxy carbene intermediates enabled by copper-catalyzed carbonylation[J]. *Green Carbon*, 2024, **2**(1): 70−80.

[9] Cao Y, Huang Y, He L. Sustainable route toward N-Boc amines: $AuCl_3$/CuI-catalyzed *N*-tert-butyloxycarbonylation of amines at room temperature[J]. *ChemSusChem*, 2022, **15**(4): e202102400.

[10] Cao Y, Yang J G, Deng Y, *et al*. Amine-responsive disassembly of AuI-CuI double salts for oxidative carbonylation[J]. *Angew Chem Int Ed*, 2020, **59**(5): 2080−2084.

[11] Cao Y, Peng Y, Cheng D, *et al*. Room-temperature co oxidative coupling for oxamide production over interfacial Au/ZnO catalysts[J]. *ACS Catal*, 2023, **13**(1): 735−743.

[12] Saliu F, Putomatti B, Rindone B. Nitrogen-containing organobases as promoters in the cobalt(II)-Schiff base catalyzed oxidative carbonylation of amines[J]. *Tetrahedron Lett*, 2012, **53**(28): 3590−3593.

[13] Mancuso R, Raut D S, Della Ca' N, *et al*. Catalytic oxidative carbonylation of amino moieties to ureas, oxamides, 2-oxazolidinones and benzoxazolones[J]. *ChemSusChem*, 2015, **8**(13): 2204−2211.

[14] Dong K, Elangovan S, Sang R, *et al*. Selective catalytic two-step process for ethylene glycol from carbon monoxide[J]. *Nat Commun*, 2016, **7**(1): 12075.

[15] Gadge S T, Bhanage B M. Pd/C-catalyzed synthesis of oxamates by oxidative cross double carbonylation of amines and alcohols under co-catalyst, base, dehydrating agent and ligand-free conditions[J]. *J Org Chem*, 2013, **78**(13): 6793−6797.

[16] Orito K, Miyazawa M, Nakamura T, *et al*. $Pd(OAc)_2$-catalyzed carbonylation of amines[J]. *J Org Chem*, 2006, **71**(16): 5951−5958.

[17] Kozo H, Yoshihito K, Koshi O, *et al*. Selective oxidative carbonylation of amines to oxamides and ureas catalyzed by palladium complexes[J]. *Bull Chem Soc Jpn*, 2004, **77**(12): 2237−2250.

[18] Wu X F, Neumann H, Beller M. Palladium-catalyzed oxidative carbonylation reactions[J]. *ChemSusChem*, 2013, **6**(2): 229−241.

[19] Meyer T, Rabeah J, Brückner A, *et al*. Visible-light-induced palladium-catalyzed dehydrogenative carbonylation of amines to oxalamides[J]. *Chem -Eur J*, 2021, **27**(18): 5642−5647.

[20] Lu L, Qiu F, Alhumade H, *et al*. Tuning the oxidative mono- or double-carbonylation of alkanes with CO by choosing a Co or Cu catalyst[J]. *ACS Catal*, 2022, **12**(15): 9664−9669.

[21] Lu B, Xu M H, Qi X T, *et al*. Switchable radical carbonylation by philicity regulation[J]. *J Am Chem Soc*, 2022, **144**(32): 14923−14935.

[22] Liu J, Dong K, Franke R, *et al*. Selective palladium-catalyzed carbonylation of alkynes: An atom-economic synthesis of 1,4-dicarboxylic acid diesters[J]. *J Am Chem Soc*, 2018, **140**(32): 10282−10288.

[23] Zhao F, Ai H J, Wu X F. Copper-catalyzed substrate-controlled carbonylative synthesis of alpha-keto amides and amides from alkyl halides[J]. *Angew Chem Int Ed*, 2022, **61**(17): e202200062.

[24] Fernández-Alvarez V M, de la Fuente V, Godard C, *et al*. Pd-catalysed mono- and dicarbonylation of aryl iodides: Insights into the mechanism and the selectivity[J]. *Chem -Eur J*, 2014, **20**(35): 10982−10989.

[25] McKillop A, Sanderson W R. Sodium perborate and sodium percarbonate: Further applications in organic synthesis[J]. *J Chem Soc Perkin Trans 1*, 2000, (4): 471−476.

[26] Wang F, Stahl S S. Electrochemical oxidation of organic molecules at lower overpotential: Accessing broader functional group compatibility with electron-proton transfer mediators[J]. *Acc Chem Res*, 2020, **53**(3): 561−574.

[27] Giannoccaro P, Tommasi I, Aresta M. Carbamoyl complexes as a source of isocyanates or carbamyl chlorides[J]. *J Organomet Chem*, 1994, **476**(1): 13−18.

[28] Dolomanov O V, Bourhis L J, Gildea R J, *et al*. OLEX2: A complete structure solution, refinement and analysis program[J]. *J Appl Crystallogr*, 2009, **42**(2): 339−341.

[29] Sheldrick G. SHELXT-integrated space-group and crystal-structure determination[J]. *Acta Crystallogr Sect A*, 2015, **71**(1): 3−8.

[30] Sheldrick G. Crystal structure refinement with SHELXL[J]. *Acta Crystallogr Sect C*, 2015, **71**(1): 3−8.

[31] Yin G, Mu X, Liu G. Palladium(II)-catalyzed oxidative difunctionalization of alkenes: Bond forming at a high-valent palladium center[J]. *Acc Chem Res*, 2016, **49**(11): 2413−2423.

[32] van Belzen R, Elsevier C J, Dedieu A, *et al*. Stereospecific reaction of molecular halogens with palladacyclopentadienes containing bidentate nitrogen ligands to give 1,4-dihalo-1,3-dienes *via* palladium(Ⅳ) intermediates[J]. *Organometallics*, 2003, **22**(4): 722−736.

[33] van Belzen R, Hoffmann H, Elsevier C J. Catalytic three-component synthesis of conjugated dienes from alkynes *via* Pd^0, Pd^{II} and Pd^{IV} intermediates containing 1,2-diimine[J]. *Angew Chem Int Ed*, 1997, **36**(16): 1743−1745.

[34] Giannoccaro P, Ferragina C, Gargano M, *et al*. Pd-catalysed oxidative carbonylation of amino alcohols to *N,N′* -bis(hydroxyalkyl) ureas under mild conditions using molecular oxygen as the oxidant[J]. *Appl Catal A-Gen*, 2010, **375**(1): 78−84.

[35] Della Ca' N, Bottarelli P, Dibenedetto A, *et al*. Palladium-catalyzed synthesis of symmetrical urea derivatives by oxidative carbonylation of primary amines in carbon dioxide medium[J]. *J Catal*, 2011, **282**(1): 120−127.

[36] Didgikar M R, Joshi S S, Gupte S P, *et al*. Oxidative carbonylation of amine using water-soluble palladium catalysts in biphasic media[J]. *J Mol Catal A- Chem*, 2011, **334**(1): 20−28.

[37] Liu J M, Peng X G, Liu J H, *et al*. Synthesis of 2-oxazolidinones by salen-Co-complexes catalyzed oxidative carbonylation of *β*-amino alcohols[J]. *Tetrahedron Lett*, 2007, **48**(6): 929−932.

[38] Gabriele B, Salerno G, Mancuso R, *et al*. Efficient synthesis of ureas by direct palladium-catalyzed oxidative carbonylation of amines[J]. *J Org Chem*, 2004, **69**(14): 4741−4750.

[39] McKillop A, Sanderson W R. Sodium perborate and sodium percarbonate: Cheap, safe and versatile oxidising agents for organic synthesis[J]. *Tetrahedron*, 1995, **51**(22): 6145−6166.

[40] Zhou L, Zhan H Y, Liu H L, *et al*. An efficient and practical process for Pd/Cu cocatalyzed homocoupling reaction of terminal alkynes using sodium percarbonate as a dual reagent in aqueous media[J]. *Chin J Chem*, 2007, **25**(10): 1413−1416.

[41] Martinelli J R, Clark T P, Watson D A, *et al*. Palladium-catalyzed aminocarbonylation of aryl chlorides at atmospheric pressure: The dual role of sodium phenoxide[J]. *Angew Chem Int Ed*, 2007, **46**(44): 8460−8463.

由钯酰胺反应性调控胺的单羰和双羰化反应合成脲和草酰胺衍生物

王锦辉[1,2], 曹彦伟[1*], 何 林[1*]

（1. 中国科学院兰州化学物理研究所 羰基合成与选择氧化国家重点实验室, 甘肃 兰州 730000;
2. 中国科学院大学, 北京 100049）

摘要: 羰基化反应可以在分子中引入羰基, 然而, 在同种底物上实现精确的选择性单或双羰基化仍是一项挑战. 因此, 我们提出了一种新策略, 通过精准控制钯酰胺的反应性来合成脲和草酰胺衍生物. 通过单晶 X 射线衍射, 我们详细揭示了钯酰胺的结构. 进一步的控制实验和循环伏安法研究帮助我们深入理解了钯酰胺在羰基化反应中, 通过氧化或插入羰基实现单羰基化或双羰基化的具体机制. 通过使用环保的过碳酸钠作为氧化剂和碱, 在常温条件下, 我们成功开发了一种由钯和碘共催化的可控羰基化体系. 该策略不仅显著提高了反应选择性, 同时也降低了传统羰基化方法可能带来的爆炸风险, 为实验室安全提供了额外的保障.

关键词: 选择性调控; 钯催化; 氧化羰基化; 胺羰基化; 绿色试剂

《分子催化 (中英文)》简介

《分子催化 (中英文)》是由中国科学院兰州化学物理研究所主办、中国科学院主管、科学出版社出版的向国内外公开发行的学术性刊物. 主要报道有关分子催化方面最新进展与研究成果. 辟有学术论文、研究简报、研究快报及综合述评等栏目. 内容侧重于配位催化、酶催化、光助催化、催化过程中的立体化学问题、催化反应机理与动力学、催化剂表面态的研究及量子化学在催化学科中的应用等. 工业催化过程中的均相催化剂、固载化学的均相催化剂、固载化的酶催化剂等活化、失活和再生; 用于新催化过程的催化剂的优选与表征等方面的内容, 本刊亦有报道. 读者对象主要是科研单位及工矿企业中从事催化工作的科技人员、研究生、高等院校化学系和化工系的师生.

《分子催化 (中英文)》已被美国化学文摘 (CA)、俄罗斯化学文摘、中国科学引文数据库、中国化学文献数据库、中国学术期刊文摘、中国化工文摘等国内外文献数据库收录.《分子催化 (中英文)》现为《中文核心期刊要目总览》的中国核心期刊和中国科技核心期刊. 曾荣获中国科学院和甘肃省科委“优秀期刊三等奖”和“优秀科技期刊”奖.

《分子催化 (中英文)》为双月刊, 每逢双月末出版, 大 16 开本, 约 16 万字, 每册定价 30.00 元. 中国标准连续出版物号：ISSN 1001−3555 / CN 62−1227 / O6. 欢迎订阅, 欢迎来稿.